ChemPhysChem

Chemistry Europe
European Chemical Societies Publishing

Accepted Article

Title: Mutual Transformations of Polysulfide Chromophore Species in Sodalite-Group minerals: A DFT Study on S6 Decomposition

Authors: Maria Fedyaeva, Sergey Lepeshkin, Nikita V. Chukanov, and Artem R. Oganov

To be cited as: *ChemPhysChem* **2024**, e202400532

Link to VoR: https://doi.org/10.1002/cphc.202400532

WILEY VCH

Mutual Transformations of Polysulfide Chromophore Species in Sodalite-Group minerals: A DFT Study on S_6 Decomposition

Maria Fedyaeva,[1,2,*] *Sergey Lepeshkin,*[1, 2, 3] *Nikita V. Chukanov*[4] *and Artem R. Oganov*[2]

[1] Vernadsky Institute of Geochemistry and Analytical Chemistry, Russian Academy of Sciences, Kosygina, 19, Moscow, 119991, Russia
[2] Skolkovo Institute of Science and Technology, Bolshoy Boulevard 30, bld. 1, Moscow 121205, Russia
[3] Lebedev Physical Institute, Russian Academy of Sciences, 53 Leninskii prosp.; 119991 Moscow, Russia
[4] Federal Research Center of Problems of Chemical Physics and Medicinal Chemistry, Russian Academy of Sciences, Chernogolovka 142432, Russia

* Maria.Fedyaeva@skoltech.ru

Abstract

It is known that various polysulfide species determine the color of sodalite-group minerals (haüyne, lazurite, and slyudyankaite), and that heating induces their transformations and color change, but the mechanisms of the transitions are unknown. A prominent example is the decay of cyclic S_6 molecule. Using density-functional simulations, we explore its main decay pathways into the most probable final reaction products (the pairs of radical anions $S_3^{\bullet-}$+ $S_3^{\bullet-}$ and $S_2^{\bullet-}$ + $S_4^{\bullet-}$). It was found that the most favorable reaction path involves initial capture of one electron by the S_6 molecule, which greatly facilitates its decay of S_6 and leads to the opening of the S_6 cycle, and subsequent decomposition of the thus formed chain radical anion, with a limiting energy barrier of ~0.4 eV. Neutral polysulfide molecules capture one electron with a significant energy reduction. The radical anions $S_n^{\bullet-}$ (n = 2 – 6) are the most stable ones among corresponding species with the same n values and different charges. The capture of the second electron by $S_6^{\bullet-}$ occurs with a huge energy barrier (~2 eV). The results of the DFT calculations are in agreement with experimental data on the products of thermal conversions of extra-framework S-bearing groups in sodalite-group minerals.

Introduction

Various polysulfide molecules, anions and radical anions have been identified as extra-framework components within structural cavities of sodalite group minerals. [1, 2] The sodalite-related minerals haüyne, lazurite, and recently discovered mineral species slyudyankaite are components of the rock lapis lazuli - which is widely used as a beautiful ornamental gemstone. Sodalite-group minerals and their synthetic analogues used as pigments are characterized by a wide variations in S-bearing extra-framework components including various polysulfide groups ($S_2^{\bullet-}$, $S_3^{\bullet-}$, $S_4^{\bullet-}$ radical anions, and neutral S_4 and S_6 particles) which are chromophores [3–5] determining different colors of these materials (blue, green, yellow or lilac: see color space chromaticity diagram for sodalite-group minerals. [6]

For example, deep blue color of the mineral lazurite is due to the presence of the $S_3^{\bullet-}$ chromophore centers. [7-10] The S_4 molecules are responsible for the red color (with purple or lilac hue if additionally trace amounts of $S_3^{\bullet-}$ are present). [4,11] Green color of sluydankaite [7] is caused by the simultaneous presence of $S_2^{\bullet-}$ and S_6 particles (yellow chromophores) and minor amounts of $S_3^{\bullet-}$ radical anions (a strong blue chromophore). Yellow color of the sodalite-group mineral bolotinaite, ideally $Na_6K(Al_6Si_6O_{24})F\cdot 4H_2O$, is caused by the admixture of $S_2^{\bullet-}$ and the absence of other chromophore centers.[12,13] Thus, understanding the role of sulfur-bearing species as chromophores helps in explaining the coloration mechanisms of various minerals. [10,14]

The occurrence of various S-bearing groups in these minerals along with specific features of their crystal structures sheds light on the conditions under which these minerals were formed, providing a deeper understanding of the geological history of host rocks . [15,16]

Negatively charged polysulfide groups are also present in some minerals belonging to other structure types. For example, the S_5^{2-} ions occur in structural cavities of the members of the bystrite–sulfhydrylbystrite solid-solution series, $(K,Na)_2Na_5Ca(Al_6Si_6O_{24})S_5^{2-}(Cl^-,HS^-)$. [17–20] In this study, we conducted comprehensive theoretical analysis of the formation of chromophore polysulfide species as a result of thermal transformations of S_6 molecules. This involves consideration of all the main decomposition pathways of the S_6 particles, including possible capture of one or two electrons.

According to the experimental data, [1, 12] the scheme of transformations of extra-framework components in SO_4^{2-}-bearing members of the sodalite group during their heating at 700 °C under reducing conditions may include the elementary processes $3SO_4^{2-} \rightarrow S_3^{\bullet-} + 5e + 6O_2(gas)$ and $6SO_4^{2-} \rightarrow S_2^{\bullet-} + S_4^{\bullet-} + 10e + 12O_2(gas)$ and $2CO_2 + 2e \rightarrow C_2O_4^{2-}$ (e = electron). Subsequent annealing in air at 800°C results in the partial reverse transformations as well as the reactions $S_4^{\bullet-} + S_2^{\bullet-} \rightarrow 2S_3^{\bullet-}$, $S_3^{\bullet-} + 5e + 6O_2(gas) \rightarrow 3SO_4^{2-}$, and $C_2O_4^{2-} \rightarrow 2CO_2(gas) + 2e$. The reduction of extra-framework water molecules in accordance with the scheme $3H_2O \rightarrow 2H_3O + ½O_2 + 2e$ could be an alternative source of electrons.

Based on the experimental data, [21- 23] it was concluded that the $S_3^{\bullet-}$ radical anion is the most stable polysulfide group. Heating of the S_6-bearing triclinic lazurite-related mineral slyudyankaite, ideally $Na_{28}Ca_4(Si_{24}Al_{24}O_{96})(SO_4)_6(S_6)_{1/3}(CO_2)\cdot 2H_2O$, [7] above 500°C results in its irreversible transformation to a sodalite-type compound with a cubic structure. [24] After heating slyudyankaite at 700°C under reducing conditions, the S_6 and SO_4^{2-} groups transform to the extra-framewotk species HS^-, $S_2^{\bullet-}$, and $S_4^{\bullet-}$. Further annealing of preheated slyudyankaite at 800°C in air results in the disappearance of HS^-, $S_2^{\bullet-}$, and $S_4^{\bullet-}$ and formation of the $S_3^{\bullet-}$ groups.[1] The $S_3^{\bullet-}$ radical anion is the only polysulfide species among products of annealing of S_4-bearing haüyne at 800°C. [12]

In this work, the energy barriers of the elementary stages in different channels of the S_6 thermal transformations were determined. Based on these data, the most likely pathways for chromophore formation were identified. Additionally, we found which particles tend to form more frequently in the minerals mentioned above. This study enhances the knowledge of coloration mechanisms in sodalite-group minerals and the role of polysulfide groups as

possible markers of the conditions of geological processes during which these minerals were formed.

Computational Methodology

In this study, the energies and geometries of the particles were calculated using the Gaussian 16 software. [25] The initial atomic structures of the cyclic S_5 ("boat" conformation) and S_6 ("armchair" conformation) molecules were taken from our previous study. [26] We utilized Gaussian's Transition State (TS) calculations to determine the intermediate states along the reaction pathways. [27] To validate found TS, we conducted Intrinsic Reaction Coordinate (IRC) calculations. [28] Based on this approach, the progression of reactions in both forward and backward directions from the obtained transition state could be thoroughly examined. The main pathway was additionally verified using the NEB[29] method in the ORCA[30] program. In all calculations we used the hybrid B3LYP functional,[31] along with the 6-311+G(d,p) basis set. [32] Previous studies showed that results of B3LYP/6-311G* calculations of the geometry and energetics of neutral and charged sulfur molecules agree with those yielded by the MP2/6-311G* level of theory[33] and experimental data.[34,26] We also calculated the vibrational spectra of particles in all states. We verified that in all local minima there are no imaginary frequencies, while in each TS only one imaginary frequency was found

Results and Discussion

DFT calculations have shown that the studied reaction of decomposition of the S_6 molecule can proceed *via* three possible scenarios: (1) decomposition of the uncharged S_6 molecule followed by the capture of electron; (2) capture of one electron with the opening of the six-membered cycle followed by decomposition with subsequent product charging; (3) charging the S_6 molecule to form first $S_6^{\bullet-}$ and thereafter S_6^{2-} and subsequent breaking of the structure into various products. The final products of the considered reaction pathways are the pairs of chromophores $S_3^{\bullet-}$ + $S_3^{\bullet-}$ and $S_4^{\bullet-}$ + $S_2^{\bullet-}$. The overall scheme showing all meaningful decomposition pathways is shown in Figure 1.

10.1002/cphc.202400532

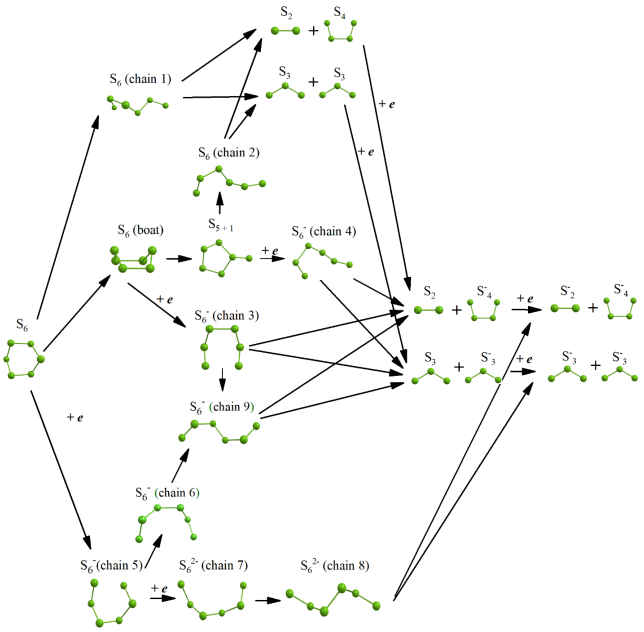

Figure 1. Overall scheme showing main decomposition pathways of the S_6 molecule. The numbering of the S_6 structures in the chain form is the same as in the figures below.

In each of these pathways the starting point is the molecule S_6 in the chair conformation. The bond lengths in this molecule are 2.12 Å, and the angles are 103.1°. The final particles are chromophore ions $S_2^{\bullet -}$, $S_3^{\bullet -}$ and $S_4^{\bullet -}$. The bond lengths are 2.05 Å; 2.04 Å, 2.00 Å, 2.28 Å and the bond angles in $S_3^{\bullet -}$ and $S_4^{\bullet -}$are 115.9° and 109.5° respectively, which is consistent with previous computational and experimental studies. [24, 29, 30] Some intermediate geometries are consistent with the data from Ref. 31. The geometries of all stable particles are given in ESI (section S1). Below, each of the scenarios is considered in more detail.

The first pathway of the scenario (1) involves the decomposition of the uncharged S_6 molecule followed by the capture of electrons. There are several possibilities for the implementation of this scenario. Let us start by considering the simplest one. In this path, initially, the uncharged S_6 molecule transforms into a chain (see Figure 2a). The barrier of this reaction stage is 1.74 eV. Next, with smaller barriers, the chain can decompose into different products both before and after capture of one electron. For example, the uncharged S_6 chain can decompose into S_4 and S_2 molecules, as demonstrated in Figure 2a. We considered it meaningless to further explore this pathway due to the very high first energy barrier, which makes the reaction unlikely.

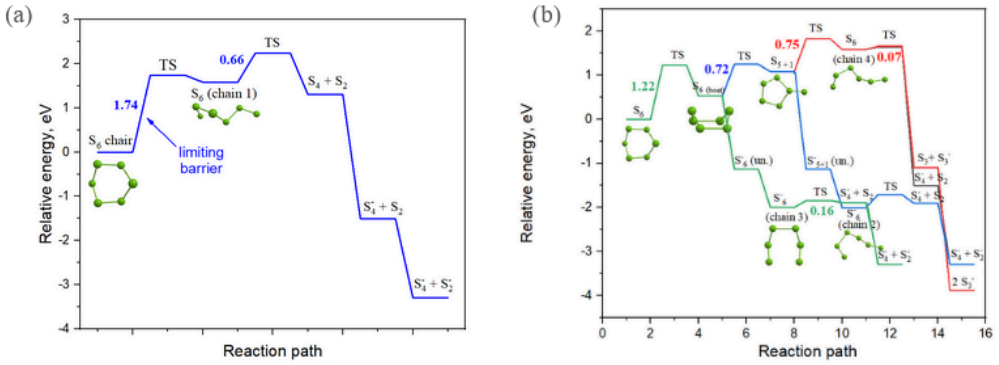

Figure 2. Decomposition of the uncharged S_6 molecule without (a) and through (b) initial conformational change from chair to boat. The numbers near to the lines on these and subsequent graphs correspond to the values of energy barriers in eV. The energy level of an unrelaxed particle at the initial moment after electron capture is marked by $S_x^{\bullet -}$(un) where x is the number of atoms in the particle. In the fork points of the reaction pathway, one of the branches is drawn in a new color.

In the second pathway of the scenario (1), the S_6 molecule in the armchair conformation undergoes a transformation to the less stable boat conformation (see Figure 2b). According to our calculations, the energy difference between these two conformations is 0.53 eV. The energy barrier for this transformation is 1.22 eV. This high barrier explains the experimental fact that in the structural cavities of the sodalite-type framework the S_6 molecules predominantly occur in the armchair conformation. [7] Let us, however, continue for a moment the discussion of the decay of the S_6 molecule in boat conformation. The S_6-boat can transform into an unusual strained five-membered ring with an attached S atom (we refer to this configuration as S_{5+1}) with the energy barrier of 0.72 eV. Thereafter S_{5+1} can further transform into a chain with an energy barrier ~ 0.75 eV and then with a very low barrier (0.07 eV) break down into two neutral molecules. There are two possible products of this reaction: S_4+S_2 or 2S_3. Subsequently, each of the particles can capture an electron without a barrier and with an energetic advantage, indicating greater stability of the charged particles.

Both for the S_6 boat conformation and for the S_{5+1} ring, the uptake of one electron is also very energetically favorable. In Figure 2b, we showed the energy levels of these molecules immediately after electron capture (unrelaxed products) and after relaxation. In the next elementary stage, one bond breaks and ring configuration transforms into a chain form. The charged particles can decompose into S_2 and $S_4^{\bullet -}$ with a very low barrier (0.16 and 0.29 respectively) or into S_3 and $S_3^{\bullet -}$ particles with significantly higher barriers (this is why it is not shown in the graph).

The S_6 molecule in the initial (armchair) configuration can also accept one electron. It is the next fundamental pathway (scenario 2, see Figure 3). In the graph, we showed the energy level corresponding to the energy of the molecule at the initial moment of electron capture (unrelaxed) and the energy of the optimized charged particle. During the optimization stage, one bond breaks and the molecule transforms into a charged chain isomer (chain 5). The overall energy decrease upon electron capture is more than 2 eV.

The subsequent most favorable pathway involves the sequential inversion of the chain 5, progressing through an intermediate local minimum (chain 6), and leading into chain 9, with corresponding energy barriers of 0.23 and 0.13 eV. Furthermore, the system can decompose into $S_4^{\bullet-}$+ S_2 or $S_3^{\bullet-}$+ S_3 reaction products with energy barriers of ~0.5 eV. Additionally, for this pathway, considered to be the most probable (since it has the smallest activation barrier), a reaction profile using free energy (ΔG) at 300 K was determined and included in the supplementary materials (section S2).

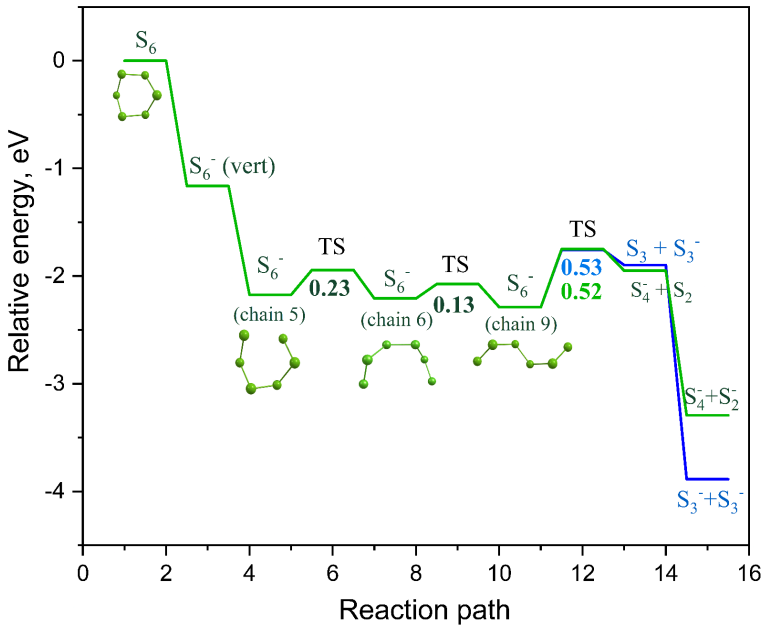

Figure 3. Reaction pathway involving capture of 1 electron by armchair S_6 molecule followed by its decomposition. The energy level corresponding to the energy of the unrelaxed $S_6^{\bullet-}$ radical anion at the initial moment of electron capture is marked by $S_6^{\bullet-}$ (un). In the fork point of the reaction pathway, one of the branches is drawn in a new color.

The third scenario involves the sequential capture of two electrons by the S_6 molecule with its further breakdown (Figure 4a). One should note that the capture of the second electron is extremely unfavorable, by nearly 2 eV. This value was determined as the difference between the energies of the molecule at the initial moment of the second electron capture and of the optimized particle with the charge of –1. The instability of S_6^{2-} makes this process unlikely. However, based on the Raman spectroscopy data, the presence of trace amounts of the S_6^{2-} anions in sodalite cages of the mineral slyudyankaite cannot be excluded [7]. For this reason, the following decomposition of S_6^{2-} has been studied.

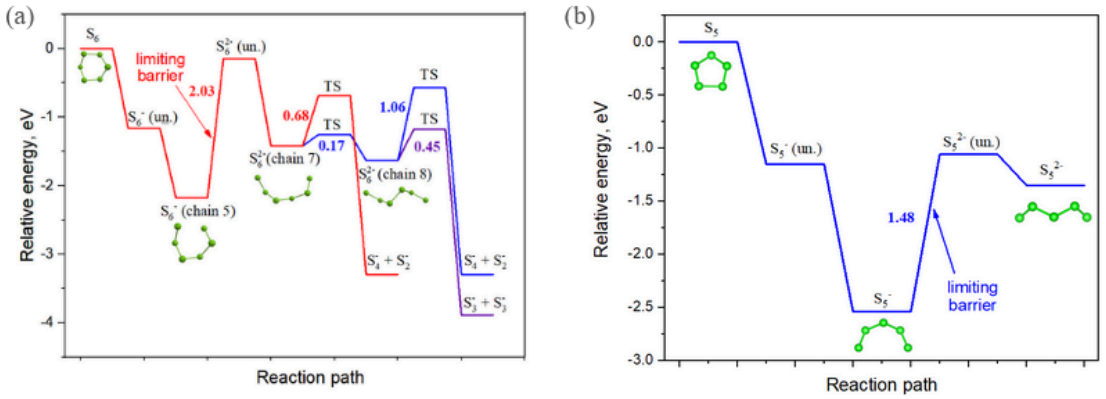

Figure 4. (a) Reaction pathway involving sequential capture of two electrons by the S_6 molecule with further breakdown, (b) Reaction pathway involving sequential capture of two electrons by the S_5 molecule. The energy levels corresponding to the energies of unrelaxed particles at the initial moment of electron capture are marked by $S_x^{\bullet-}$ (un) or S_x^{2-} (un), where x is the number of atoms in a particle. In the fork points of the reaction pathway, one of the branches is drawn in a new color.

During the optimization of the S_6^{2-} anion, the chain changes its shape with energy decrease of 1.22 eV. Further transition to the chain of another conformation (with the barrier of 0.17 eV) and its subsequent decay into $S_4^{\bullet-} + S_2^{\bullet-}$ (barrier 1.06 eV) or $S_3^{\bullet-} + S_3^{\bullet-}$ (barrier 0.45 eV) is the most favorable path. It can be noted that the energy of $S_3^{\bullet-} + S_3^{\bullet-}$ is lower than the energy of $S_4^{\bullet-} + S_2^{\bullet-}$ (by 0.59 eV).

Additionally, we studied the process of electron capture by S_5 molecules, since, as noted above, the S_5^{2-} ions occur in structural cavities of some minerals belonging to the cancrinite group which is related to the sodalite group [19, 20] (see Figure 4b). The charging process is similar to those for S_6 molecules. At the first moment after the electron capture, the energy decrease is 1.15 eV. During the optimization process, the $S_5^{\bullet-}$ radical anion transforms into a chain with further energy reduction of 1.39 eV. The capture of a second electron occurs with the energy barrier of 1.48 eV, which is lower than the corresponding barrier for the S_6 molecule.

Conclusions

A systematic study of mutual transformations of chromophore polysulfide species (neutral molecules, radical anions and anions) has been carried out starting from the S_6 molecule. These particles are crucial components in determining the colors of sodalite group minerals such as haüyne, lazurite, and slyudyankaite, as well as important markers of the conditions under which their host rocks were formed. This involves determination of various decomposition pathways of the S_6 molecule. At any stage of these paths the system can get additional electrons from external sources. We found that getting one electron is favorable, but getting two electrons is not (explaining why S_6^{2-} anions in sodalite-group minerals have not been found in any significant quantities). As all bonding molecular orbitals in cyclic S_n molecules are fully occupied, the extra electron goes into an antibonding orbital and inducing a barrierless opening of the S_n ring. Electrons thus act as "scissors", cutting covalent S-S

bonds. The final products of decay of S_6^- are the pairs of radical anions, $S_3^{\bullet-} + S_3^{\bullet-}$ or $S_2^{\bullet-} + S_4^{\bullet-}$, and in both cases the limiting energy barrier is ~0.4 eV. These pairs of radical anions are thermodynamically more stable than the original S_6 molecule (with $S_3^{\bullet-} + S_3^{\bullet-}$ being the most stable), but the decay of S_6 requires an electron source (to reduce the barriers and stabilize decomposition products) and temperature (to overcome the activation barrier of 0.4 eV). Our findings confirm that electron capture is a spontaneous process followed by a significant energy reduction. In addition, the radical anions $S_n^{\bullet-}$ (n = 2 – 6) are the most stable ones among corresponding particles with different charges.

Acknowledgements

Global structure optimization was supported by the Russian Science Foundation (Grant 19-72-30043). The calculations were performed on Oleg and Arkuda supercomputers at Skoltech and at the Joint Supercomputer Center of the Russian Academy of Sciences. The stability analysis was performed within the Project of the State Assignment (Vernadsky Institute of Geochemistry and Analytical Chemistry of Russian Academy of Sciences, Moscow, Russia). The comparison of the results of DFT calculations with experimental data was carried out in accordance with the state task, registration number 124013100858-3 (for N.V.C.). The authors thank Alexey Maltsev for valuable discussions.

References

1 N. V. Chukanov, R. Y. Shendrik, M. F. Vigasina, I. V. Pekov, A. N. Sapozhnikov, V. D. Shcherbakov and D. A. Varlamov, Crystal chemistry, isomorphism, and thermal conversions of extra-framework components in sodalite-group minerals, *Minerals (Basel)*, 2022, **12**, 887.

2 R. Steudel and T. Chivers, The role of polysulfide dianions and radical anions in the chemical, physical and biological sciences, including sulfur-based batteries, *Chem. Soc. Rev.*, 2019, **48**, 3279–3319.

3 I. Gayday, A. Teplukhin and D. Babikov, Computational analysis of vibrational modes in tetra-sulfur using dimensionally reduced potential energy surface, *Mol. Phys.*, 2019, **117**, 2546–2558.

4 P. Rejmak, Computational refinement of the puzzling red tetrasulfur chromophore in ultramarine pigments, *Phys. Chem. Chem. Phys.*, 2020, **22**, 22684–22698.

5 B. Eckert and R. Steudel, in *Topics in Current Chemistry*, Springer Berlin Heidelberg, Berlin, Heidelberg, 2012, pp. 31–98.

6 N. V. Chukanov, R. Y. Shendrik, M. F. Vigasina, I. V. Pekov, A. N. Sapozhnikov, V. D. Shcherbakov and D. A. Varlamov, Crystal chemistry, isomorphism, and thermal conversions of extra-framework components in sodalite-group minerals, *Minerals (Basel)*, 2022, **12**, 887.

7 A. N. Sapozhnikov, N. B. Bolotina, N. V. Chukanov, R. Y. Shendrik, E. V. Kaneva, M. F. Vigasina, L. A. Ivanova, V. L. Tauson and S. V. Lipko, Slyudyankaite, Na28Ca4(Si24Al24O96)(SO4)6(S6)1/3(CO2)·2H2O, a new sodalite-group mineral from the Malo-Bystrinskoe lazurite deposit, Baikal Lake area, Russia, *Am. Mineral.*, 2023, **108**, 1805–1817.

8 A. N. Sapozhnikov, V. L. Tauson, S. V. Lipko, R. Y. Shendrik, V. I. Levitskii, L. F.

Suvorova, N. V. Chukanov and M. F. Vigasina, On the crystal chemistry of sulfur-rich lazurite, ideally Na7Ca(Al6Si6O24)(SO4)(S3)–·nH2O, *Am. Mineral.*, 2021, **106**, 226–234.

9 N. V. Chukanov, R. Y. Shendrik, M. F. Vigasina, I. V. Pekov, A. N. Sapozhnikov, V. D. Shcherbakov and D. A. Varlamov, Crystal chemistry, isomorphism, and thermal conversions of extra-framework components in sodalite-group minerals, *Minerals (Basel)*, 2022, **12**, 887.

10 T. Chivers and P. J. W. Elder, Ubiquitous trisulfur radical anion: fundamentals and applications in materials science, electrochemistry, analytical chemistry and geochemistry, *Chem. Soc. Rev.*, 2013, **42**, 5996–6005.

11 A. N. Sapozhnikov, V. L. Tauson, S. V. Lipko, R. Y. Shendrik, V. I. Levitskii, L. F. Suvorova, N. V. Chukanov and M. F. Vigasina, On the crystal chemistry of sulfur-rich lazurite, ideally Na7Ca(Al6Si6O24)(SO4)(S3)–·nH2O, *Am. Mineral.*, 2021, **106**, 226–234.

12 N. V. Chukanov, N. V. Shchipalkina, R. Y. Shendrik, M. F. Vigasina, V. L. Tauson, S. V. Lipko, D. A. Varlamov, V. D. Shcherbakov, A. N. Sapozhnikov, A. V. Kasatkin, N. V. Zubkova and I. V. Pekov, Isomorphism and mutual transformations of S-bearing components in feldspathoids with microporous structures, *Minerals (Basel)*, 2022, **12**, 1456.

13 N. V. Chukanov, N. V. Zubkova, C. Schäfer, I. V. Pekov, R. Y. Shendrik, M. F. Vigasina, D. I. Belakovskiy, S. N. Britvin, V. O. Yapaskurt and D. Y. Pushcharovsky, Bolotinaite, ideally $(Na_7\square)(Al_6Si_6O_{24})F\cdot 4H_2O$, a new sodalite-group mineral from the Eifel palaeovolcanic region, Germany, *Mineral. Mag.*, 2022, **86**, 920–928.

14 N. V. Chukanov, R. Y. Shendrik, M. F. Vigasina, I. V. Pekov, A. N. Sapozhnikov, V. D. Shcherbakov and D. A. Varlamov, Crystal chemistry, isomorphism, and thermal conversions of extra-framework components in sodalite-group minerals, *Minerals (Basel)*, 2022, **12**, 887.

15 Y. Li, Y. Li, Y. Liu, Y. Wu, J. Wu, B. Wang, H. Ye, H. Jia, X. Wang, L. Li, M. Zhu, H. Ding, Y. Lai, C. Wang, J. Dick and A. Lu, Photoreduction of inorganic carbon(+IV) by elemental sulfur: Implications for prebiotic synthesis in terrestrial hot springs, *Sci Adv*, , DOI:10.1126/sciadv.abc3687.

16 Y. Li, H. Ye, R. Yin, Z. Hu, J. Zhu, Y. Du, H. Ding, Y. Lai, C. Wang, A. Lu and Y. Li, Unpaired electrons-induced geochemical activity of native sulfur in energy-triggered ring-opening process, *Geochim. Cosmochim. Acta*, 2023, **348**, 355–368.

17 N. V. Chukanov, R. Y. Shendrik, M. F. Vigasina, I. V. Pekov, A. N. Sapozhnikov, V. D. Shcherbakov and D. A. Varlamov, Crystal chemistry, isomorphism, and thermal conversions of extra-framework components in sodalite-group minerals, *Minerals (Basel)*, 2022, **12**, 887.

18 A. N. Sapozhnikov, E. V. Kaneva, L. F. Suvorova, V. I. Levitsky and L. A. Ivanova, Sulfhydrylbystrite, Na5K2Ca(Al6Si6O24)(S5)(SH), a new mineral with the LOS framework, and re-interpretation of bystrite: cancrinite-group minerals with novel extra-framework anions, *Mineral. Mag.*, 2017, **81**, 383–402.

19 A. N. Sapozhnikov, E. V. Kaneva, L. F. Suvorova, V. I. Levitsky and L. A. Ivanova, Sulfhydrylbystrite, Na5K2Ca(Al6Si6O24)(S5)(SH), a new mineral with the LOS framework, and re-interpretation of bystrite: cancrinite-group minerals with novel extra-framework anions, *Mineral. Mag.*, 2017, **81**, 383–402.

20 N. V. Chukanov, A. N. Sapozhnikov, E. V. Kaneva, D. A. Varlamov and M. F. Vigasina, Bystrite, $Na_7Ca(Al_6Si_6O_{24})S_5^{2-}Cl^-$: formula redefinition and relationships with other four-layer cancrinite-group minerals, *Mineral. Mag.*, 2023, **87**, 455–464.

21 G. S. Pokrovski and L. S. Dubrovinsky, The S3- ion is stable in geological fluids at

elevated temperatures and pressures, *Science*, 2011, **331**, 1052–1054.
22 G. S. Pokrovski and J. Dubessy, Stability and abundance of the trisulfur radical ion S3− in hydrothermal fluids, *Earth Planet. Sci. Lett.*, 2015, **411**, 298–309.
23 Ivanov V.G., Sapozhnikov A.N. Lazurites of the USSR. Nauka, Novosibirsk, 1985, 173 pp. (in Russian)
24 M. J. Frisch, G. W. Trucks, H. B. Schlegel, G. E. Scuseria, M. A. Robb, J. R. Cheeseman, G. Scalmani, V. Barone, G. A. Peters-son, H. Nakatsuji, X. Li, M. Caricato, A. V. Marenich, J. Bloino, B. G. Janesko, R. Gomperts, B. Mennucci, H. P. Hratchian, J. V. Ortiz, A. F. Izmaylov, J. L. Sonnenberg, D. Williams-Young, F. Ding, F. Lipparini, F. Egidi, J. Goings, B. Peng, A. Petrone, T. Henderson, D. Ranasinghe, V. G. Zakrzewski, J. Gao, N. Rega, G. Zheng, W. Liang, M. Hada, M. Ehara, K. Toyota, R. Fukuda, J. Hasegawa, M. Ishida, T. Nakajima, Y. Honda, O. Kitao, H. Nakai, T. Vreven, K. Throssell, J. A. Montgomery, Jr., J. E. Peralta, F. Ogliaro, M. J. Bearpark, J. J.Heyd, E. N. Brothers, K. N. Kudin, V. N. Staroverov, T. A. Keith, R. Kobayashi, J. Normand, K. Raghavachari, A. P. Ren-dell, J. C. Burant, S. S. Iyengar, J. Tomasi, M. Cossi, J. M.Millam, M. Klene, C. Adamo, R. Cammi, J. W. Ochterski, R. L. Martin, K. Morokuma, O. Farkas, J. B. Foresman and D. J. Fox, Gaussian 16 Revision C.01, Gaussian Inc., Wallingford CT, 2016.
25 D. K. Singh, S. Das and A. Materny, *Advances in Spectroscopy: Molecules to Materials: Proceedings of NCASMM 2018*, Springer Nature, 2019.
26 M. Fedyaeva, S. Lepeshkin and A. R. Oganov, Stability of sulfur molecules and insights into sulfur allotropy, *Phys. Chem. Chem. Phys.*, 2023, **25**, 9294–9299.
27 J. L. Durant, Evaluation of transition state properties by density functional theory, *Chem. Phys. Lett.*, 1996, **256**, 595–602.
28 K. Fukui, The path of chemical reactions - the IRC approach, *Acc. Chem. Res.*, 1981, **14**, 363–368.
29 G. Henkelman, B. P. Uberuaga and H. Jónsson, A climbing image nudged elastic band method for finding saddle points and minimum energy paths, *J. Chem. Phys.*, 2000, **113**, 9901–9904.
30 F. Neese, The ORCA program system, *Wiley Interdiscip. Rev. Comput. Mol. Sci.*, 2012, **2**, 73–78.
31 M. E. Casida, C. Jamorski, K. C. Casida and D. R. Salahub, Molecular excitation energies to high-lying bound states from time-dependent density-functional response theory: Characterization and correction of the time-dependent local density approximation ionization threshold, *J. Chem. Phys.*, 1998, **108**, 4439–4449.
32 P. J. Stephens, F. J. Devlin, C. F. Chabalowski and M. J. Frisch, Ab initio calculation of vibrational absorption and circular dichroism spectra using density functional force fields, *J. Phys. Chem.*, 1994, **98**, 11623–11627.
33 J. Cioslowski, A. Szarecka and D. Moncrieff, Conformations and thermodynamic properties of sulfur homocycles. 1. The S5, S6, S7, and S8 molecules, *J. Phys. Chem. A*, 2001, **105**, 501–505.
34 Y. Jin, G. Maroulis, X. Kuang, L. Ding, C. Lu, J. Wang, J. Lv, C. Zhang and M. Ju, Geometries, stabilities and fragmental channels of neutral and charged sulfur clusters: Sn(Q) (n = 3-20, Q = 0, ±1), *Phys. Chem. Chem. Phys.*, 2015, **17**, 13590–13597.
35 C. -K.Wang, A new global search for the ground state structure of small cluster: application to S6, Nanobiotechnology 4, **2013**, 357–366.